A Reversible, Isosymmetric, High-Pressure Phase Transition in Na_3MnF_6

Stefan Carlson,*,† Yiqiu Xu,† Ulf Hålenius,‡ and Rolf Norrestam†

Structural Chemistry, Arrhenius Laboratory, Stockholm University, SE-10691 Stockholm, Sweden, and Department of Mineralogy, Swedish Museum of Natural History, P.O. Box 50007, SE-10405 Stockholm, Sweden

Received September 13, 1997

The crystal structure of Na_3MnF_6 has been investigated at high pressures by means of single-crystal x-ray diffraction, and its Mn(III) coordination environment has been studied by means of single-crystal optical absorption spectroscopy using diamond anvil techniques. Compressibility data (unit cell parameters) were collected in the pressure range from ambient to 4.06 GPa, and structural refinements based on single-crystal diffraction data were performed at 0.12, 0.91, 2.27, and 2.79 GPa. The monoclinic space group symmetry ($P2_1/n$) is retained in the entire pressure range, but, at increasing pressure, a discontinuous phase transition is observed at ∼2.2 GPa. This is interpreted as an effect of a reversible, isosymmetric phase transition with a hysteresis width of 0.5 GPa, observed when the pressure is successively lowered. The structure refinements show that the phase transition involves a reorientation of the static prolate distortion of the coordination around manganese(III). The angle between the elongation axis (z) of the MnF_6^{3-} octahedron with [0 0 1] flips from ∼20° at ambient pressures to ∼70° at 2.79 GPa. Polarized single-crystal absorption spectra of Na_3MnF_6 show drastic changes of the polarization of bands due to spin-allowed d−d transitions in Mn(III) when passing the transition pressure, which confirm the results of the single-crystal structure refinements. A possible explanation for this transition is discussed in terms of structure packing arguments. The isothermal bulk modulus at ambient pressure and its pressure derivative were determined to $B_0 = 47.8(1)$ GPa and $B_0' = 1.2(1)$, respectively.

Introduction

The crystal structure of Na_3MnF_6, with unit cell parameters $a = 5.4709(9)$, $b = 5.6830(6)$, and $c = 8.0734(12)$ Å, $\beta = 88.964(7)°$, space group symmetry $P2_1/n$, and $Z = 2$, has previously been determined by English et al.[1] This cryolite type structure may be visualized as a distorted perovskite structure (Figure 1) composed of corner-connected alternating MnF_6^{3-} and NaF_6^{5-} octahedra, with additional eight-coordinated Na atoms located interstitially to the octahedra. The Mn coordination octahedra display two long apical Mn−F bonds and four shorter equatorial Mn−F distances, which is the common geometry for six-coordinated Mn(III) ions and is ascribed to effects due to the electronic $3d^4$ configuration, which is prone to distort the octahedral coordination due to the static Jahn−Teller effects. The elongation axis of the Mn octahedron is tilted ∼20° with respect to [0 0 1]. In this cryolite structure, the Mn(III)-centered six-coordinated sites are quasi-isolated from each other, as they share coordination elements only with adjacent NaF_6 and NaF_8 polyhedra. Consequently, cooperative Jahn−Teller distortions are expected to be reduced in this structure.

The low-charge monovalent sodium ion is anticipated to have a higher compressibility than the trivalent manganese ion. In an oversimplified manner, the sodium atoms may thus be considered as constituents of an internal pressure transmitting medium. In fact, this makes the present compound a very good candidate for studies of the high-pressure dependence of the static Jahn−Teller distortions on the coordination sphere of Mn(III). A study on the pressure dependence of deuterated ammonium hexaaquacopper(II) sulfate (Tutton's salt) has previously been reported, exhibiting a pressure-induced phase transition below 0.15 GPa, which was ascribed to a reorientation of the Jahn−Teller distortions around the copper atom.[2,3] The present investigation reports the first example of a related transition for a Mn^{3+} compound.

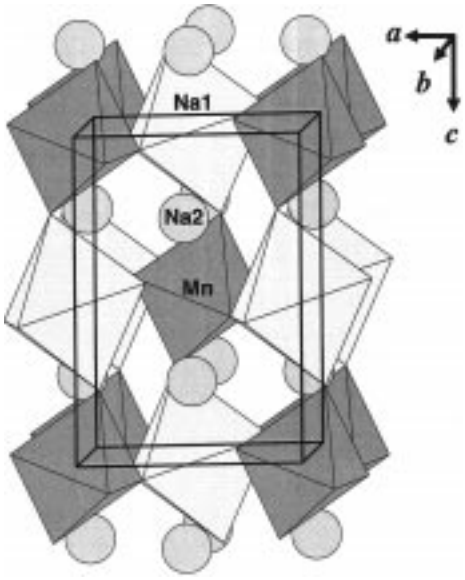

Figure 1. Na_3MnF_6 structure viewed roughly along [0 1 0], with dark octahedra indicating the manganese−fluorine coordination polyhedron. Light octahedra represents the six-coordinated Na1 atoms, and the eight-coordinated Na2 atoms are drawn as spheres.

* Author for correspondence.
† Stockholm University.
‡ Swedish Museum of Natural History.

(1) English, U.; Massa, W.; Tressaud, A. *Acta Crystallogr.* **1992**, *C48*, 6−8.

S0020-1669(97)01171-3 CCC: $15.00
Published on Web 03/14/1998

This study is part of a research program aiming at high-pressure investigations of transition metal oxides and fluorides.

Experimental Section

Synthesis. Stoichiometric mixtures of dried NaF (Merck, no. 6449) and MnF_3 (Aldrich, no. 33.929-6) were cogrinded inside a glovebox under Ar atmosphere and placed in a gold tube, which was subsequently sealed and inserted into an autoclave of stainless steel. This steel bomb was filled with water, heated to 500 °C at an external pressure of 0.25 GPa, and kept under these conditions for another 24 h. Finally, slow cooling to room temperature was achieved by simply turning the furnace off. Characterization of the synthetic products was performed by Guinier x-ray powder techniques, and the obtained powder diffraction pattern was compared to calculated powder diffraction patterns, using parameters from English et al.[1] Single-crystal photographic techniques (deJong and precession methods) were utilized to select crystals of suitable size and shape for the subsequent high-pressure experiments.

High-Pressure Equipment. The single-crystal high-pressure experiments were carried out with a Merril−Bassett type[4] diamond anvil cell (Diacell Products DXR-5 cell), equipped with type IA diamonds with anvil face diameters of 600 μm. A mixture of methanol, ethanol, and water in volume proportions of 16:3:1 was used as a hydrostatic pressure-transmitting medium. Gaskets cut out from 400-μm-thick foils of cold-rolled stainless steel (type no. SS 142331-44) were used. Pressure compartments for housing pressure medium, sample, and pressure-indicating substances were created by drilling centered holes with diameters of 300 μm in preindented gaskets using a simple, in-house-designed drilling jig. Experiment pressures were determined by measurement of the ruby fluorescence line at 694.1 nm from small (<20 μm), synthetic Cr^{3+}-doped corundum (α-Al_2O_3) crystals placed in the gasket compartment adjacent to the sample. Within the present pressure range, a linear shift is assumed, and the pressure constant[5] is 2.74 GPa nm^{-1}. The appropriate part of the ruby fluorescence spectrum was measured with a PC-controlled assembly consisting of a 25-mW Ar laser (Laser Graphics) and a spectrograph (Oriel Multispec) equipped with a 1024 diode array detector (Oriel InstaSpec II). The estimated standard deviation of the determined wavelength shift is 0.01 nm, and the estimated error of 0.016 GPa nm^{-1} in the proportionality constant (2.740) has been considered when calculating the esd's (σ's) for the different pressures. To confirm stable experimental conditions, the cell pressure was monitored immediately prior to and directly after each x-ray and optical absorption experiment. Tests with glycerine as pressure-transmitting medium were also performed to control, if possible, reactions between the methanol, ethanol, and water mixture and the sample that occur during compression. No evidence of reactions with the medium was observed.

X-ray Studies. Single-crystal x-ray intensity data were collected using a four-circle diffractometer (Siemens P4/RA) equipped with a high-speed scintillation detector (Siemens FSD), using graphite-monochromatized Mo Kα radiation (λ = 0.710 73 Å at T = 293 K) from a rotating anode generator (Siemens M18XHF). The generator was operated at 5.0 kW (50 kV and 100 mA), for a filament size of 0.3 mm × 3 mm and a collimator with diameter ϕ_i = 350 μm. Single-crystal x-ray diffraction data collection was performed with ω,2θ scans at azimuthal angles (Ψ values) selected to minimize absorption from the pressure cell. To achieve this, computer programs that generate optimal setting angles (ω_Ψ, θ_Ψ, φ_Ψ, χ_Ψ) of all possible reflections directly from the orientation matrix of the crystal were developed.[6] To reduce some of the limitations of the Siemens diffractometer software, single-point "Ψ-data collections" were made for the angular settings at the best $\Psi = 0°$ value, modulo 30°. The criterion for significance of the intensities was $F_o \geq 2\sigma_F$, and numerical absorption corrections were performed for the single crystal (size 140 × 140 × 80 μm^3) at the different pressures. Full-matrix least-squares structure refinements (minimizing $\sum w(\Delta F)^2$, $w = (\sigma_F^2 + 0.0005F^2)^{-1}$) using isotropic displacement parameters were carried out for each pressure data set.

Table 1. Compressibility Data for Na_3MnF_6[a]

P (GPa)	a (Å)	b (Å)	c (Å)	β (deg)	V (Å^3)
0.00(3)	5.4687(15)	5.6760(17)	8.070(2)	88.92(1)	250.47(18)
0.00(3)	5.465(4)	5.679(4)	8.084(3)	88.98(6)	250.9(3)
0.27(3)	5.463(4)	5.670(5)	8.063(7)	89.17(7)	249.7(4)
0.54(3)	5.437(3)	5.666(3)	8.035(3)	88.96(4)	247.51(19)
0.69(3)	5.441(2)	5.658(3)	8.030(4)	89.12(4)	247.2(2)
0.90(3)	5.421(5)	5.667(3)	8.010(3)	89.05(5)	246.0(2)
0.93(3)*	5.429(2)	5.650(2)	8.011(3)	89.15(4)	245.7(2)
1.15(3)	5.414(4)	5.652(2)	7.988(3)	89.09(4)	244.38(17)
1.42(4)*	5.4071(19)	5.641(2)	7.968(3)	89.28(4)	243.01(17)
1.45(4)	5.405(6)	5.642(5)	7.976(5)	89.04(6)	243.2(4)
1.55(4)*	5.394(5)	5.652(4)	7.972(7)	89.09(5)	243.0(3)
1.75(4)	5.402(4)	5.646(3)	7.953(3)	89.27(6)	242.51(19)
1.89(4)*	5.407(2)	5.697(3)	7.827(3)	90.64(2)	241.1(2)
1.95(4)	5.380(2)	5.6360(12)	7.926(3)	89.27(1)	240.29(13)
2.08(4)	5.377(4)	5.639(2)	7.916(5)	89.31(3)	240.0(2)
2.16(4)	5.388(2)	5.639(2)	7.921(4)	89.49(3)	240.6(2)
2.25(4)*	5.396(2)	5.694(2)	7.794(3)	90.74(2)	239.4(2)
2.27(4)	5.399(2)	5.695(3)	7.802(4)	90.66(4)	239.9(2)
2.36(5)	5.387(2)	5.690(2)	7.779(3)	90.74(3)	238.4(3)
2.49(5)	5.3876(18)	5.687(2)	7.775(4)	90.78(3)	238.2(2)
2.52(5)*	5.3810(19)	5.684(2)	7.763(3)	90.80(3)	237.42(19)
2.96(6)	5.372(2)	5.678(4)	7.746(4)	90.93(2)	236.2(2)
3.34(6)	5.342(4)	5.677(2)	7.730(5)	90.85(4)	234.4(2)
3.73(7)	5.343(2)	5.6693(14)	7.698(3)	90.89(1)	233.17(13)
4.06(7)	5.327(4)	5.646(5)	7.680(4)	90.84(4)	231.0(2)

[a] Data for pressures marked with an asterisk were collected when lowering the pressure.

All structure refinements were made using the SHELXTL PC software package.[7] Atomic scattering factors for neutral atoms from the International Tables of Crystallography[8] were applied. Additional experimental details and resulting fractional coordinates from the high-pressure structure refinements are summarized in Tables 2 and 3. Geometric calculations, compiled in Table 4, were performed with the computer programs PLATON[9] and VOLCAL.[10] The two-dimensional structure projections were made using the ATOMS program.[11]

Optical Absorption Measurements. Polarized single-crystal absorption spectra were obtained with a PC-controlled Zeiss

(2) Simmons, C. J.; Hitchman, M. A.; Stratemeier, H.; Schultz, A. J. *J. Am. Chem. Soc.* **1993**, *115*, 11304−11311.
(3) Rauw, W.; Ahsbahs, H.; Hitchman, M.; Lukin, S.; Reinen, D.; Schultz, A. J.; Simmons, C. J.; Stratmeier, H. *Inorg. Chem.* **1996**, *35*, 1902−1911.
(4) Merrill, L.; Bassett, W. A. *Rev. Sci. Instrum.* **1974**, *45*, 290.
(5) Piermarini, G. J.; Block, S.; Barnett, J. D.; Forman, A. *J. Appl. Phys.* **1975**, *46*, 2774−2780.
(6) Norrestam, R. Manuscript in preparation.
(7) SHELXTL PC, release 4.1; Siemens Analytical x-ray Instruments Inc., Madison, WI, 1990.
(8) *International Tables for x-ray Crystallography*; Kynoch Press: Birmingham, 1974; Vol. IV.
(9) Spek, A. L. PLATON, Program for the analysis of molecular geometry; University of Utrecht, Utrecht, The Netherlands, 1990.
(10) Finger, L. W. VOLCAL, Program to Calculate Polyhedral Volumes and Distortions; Carnegie Institution of Washington, Geophysical Laboratory, Washington, DC, 1971.
(11) Dowty, E. ATOMS, a computer program for displaying atomic structures; Eric Dowty, 521 Hidden Valley Rd., Kingsport, TN, 1989.

Table 2. Experimental Details for the High-Pressure Structure Determinations of Na_3MnF_6

	pressure (GPa)			
	0.12	0.91	2.27	2.79
unit cell dimensions				
a, Å	5.470(3)	5.431(3)	5.409(3)	5.386(3)
b, Å	5.690(1)	5.669(2)	5.698(2)	5.690(3)
c, Å	8.066(2)	7.992(2)	7.819(3)	7.783(3)
β, deg	89.08(4)	89.25(5)	90.44(6)	90.76(6)
unit cell volume, *V*, Å^3	251.04(14)	246.01(18)	240.98(14)	238.5(2)
density (calcd), d_x, g cm^{-3}	3.15	3.21	3.28	3.31
maximum $\sin(\theta)/\lambda$	0.70	0.70	0.70	0.70
collected reflections	505	513	513	509
unique reflections	203	200	191	192
observed reflections	124	117	125	111
linear absorption coeff	2.93	2.99	3.05	3.08
transmission factor range	0.67−0.80	0.67−0.80	0.66−0.79	0.66−0.79
no. of refined params	19	19	19	19
R^a for observed reflns	0.051	0.076	0.079	0.067
wR^b for observed reflns	0.050	0.059	0.062	0.046
max and min of $\|\Delta\|/\sigma$	<0.001	<0.001	<0.001	<0.001
max and min of $\Delta\rho$	0.51, −0.40	0.94, −0.94	0.79, −1.06	0.74, −0.99

[a] $R = \sum||F_o| - |F_c||/\sum|F_o|$. [b] $wR = [\sum w(|F_o| - |F_c|)^2/\sum w(F_o^2)]^{1/2}$.

Table 3. Fractional Atomic Coordinates and Isotropic Thermal Displacement Parameters (Å^2) with Esd's for the Na_3MnF_6 Structure

		pressure (GPa)			
		0.12	0.91	2.27	2.79
Mn	*x*	0	0	0	0
	y	0	0	0	0
	z	0	0	0	0
	U_{iso}	0.0100(7)	0.0101(9)	0.0121(8)	0.0123(8)
Na1	*x*	0	0	0	0
	y	0	0	0	0
	z	$^1/_2$	$^1/_2$	$^1/_2$	$^1/_2$
	U_{iso}	0.0141(14)	0.019(2)	0.0172(16)	0.0167(15)
Na2	*x*	0.506(3)	0.510(4)	0.517(4)	0.513(4)
	y	−0.0558(8)	−0.0574(11)	−0.0609(10)	−0.0626(10)
	z	0.2502(8)	0.2495(9)	0.2476(9)	0.2469(8)
	U_{iso}	0.0250(13)	0.0264(17)	0.0259(16)	0.0261(14)
F1	*x*	0.129(3)	0.104(6)	0.123(5)	0.112(5)
	y	0.0586(11)	0.0557(15)	0.0539(14)	0.0558(12)
	z	0.2320(8)	0.2329(10)	0.2270(10)	0.2277(9)
	U_{iso}	0.0151(18)	0.021(3)	0.018(2)	0.020(2)
F2	*x*	−0.288(4)	−0.271(5)	−0.273(5)	−0.267(4)
	y	0.1720(14)	0.1725(15)	0.1726(17)	0.1734(18)
	z	0.0539(10)	0.0541(10)	0.0486(12)	0.0494(11)
	U_{iso}	0.0239(23)	0.020(3)	0.024(3)	0.026(3)
F3	*x*	0.162(4)	0.162(5)	0.164(5)	0.172(3)
	y	0.2776(12)	0.2807(15)	0.2851(17)	0.2880(14)
	z	−0.0672(11)	−0.0689(12)	−0.0711(13)	−0.0734(10)
	U_{iso}	0.0208(19)	0.020(2)	0.026(2)	0.018(2)

MPM800 microscope−photospectrometer, using a 75-W xenon arc lamp as light source and a photomultiplier (Hamamatsu R952) as detector. Monochromatic radiation was obtained by means of a holographic concave grating, and polarized light was achieved by means of a Glan−Thompson calcite prism. Common to all measurements in the UV−vis spectral range were scans performed at 0.5-nm steps, a spectral slit of 1 nm, and data collection in three cycles. UV-transparent Zeiss 10× Ultrafluar lenses served as condensor and objective in all measurements, and the illumination and measuring spots were 100 and 60 μm, respectively. Absorption spectra in the range 333−2000 nm (30000−5000 cm^{-1}) were recorded along all three principal vibration directions (*X*, *Y*, *Z*) at ambient conditions on two single crystals (t = 36 μm) mounted in glycerine between two quartz glass slides. In addition to this, $E||Z(a)$ and $E||X'(c')$ spectra were obtained in the spectral range 400−800 nm (25 000−12 500 cm^{-1}) on a single crystal (t = 80 μm) loaded in the high-pressure cell. This crystal was measured at three different stages (at ambient conditions prior to application of high pressure, at 2.4 GPa, and after a pressure release to 0.08 GPa), and x-ray diffraction measurements were carried out between the stages to ensure that the crystal retained its orientation with respect to the anvil faces. The reference medium for the measurements of the cell-mounted crystal was the diamond anvils and the pressure-transmitting mixture. The intrisic optical absorption of type IA diamonds precluded recordings of reasonable quality outside the limited spectral range mentioned above. The obtained polarized absorption spectra were deconvoluted into partly overlapping Gaussian band components using the PeakFit 4.0 computer program.[12]

Results and Discussion

From the data illustrated in Figure 2 and compiled in Table 1, it is evident that the Na_3MnF_6 undergoes a reversible phase transition when the pressure is increased to approximately 2.2 GPa. At this pressure, the dimensions of the unit cell axes and the β-angle change abruptly, while the unit cell volume apparently remains linearly dependent on the pressure. The phase transition shows a hysteresis of about 0.4−0.6 GPa (Figure 3). The space group symmetry ($P2_1/n$) seems to be retained when passing the transition pressure. A phase transition of this character, involving a structural change with invariant space group symmetry, may be regarded as an isosymmetric phase transition.[13] The relative change of the unit cell dimensions in the pressure range from ambient conditions to 4.06 GPa is largest for the *c*-axis, intermediate for the *a*-axis, and smallest for the *b*-axis. This scheme is consistent with the packing arrangement (Figure 4) of the larger and low-charged fluorine and sodium ions. These ions are located in layers stacked in the [1 0 $\bar{3}$] direction, which would result in compressibility that is high along *c*, lower along *a*, and lowest along *b*. Over about 4.0 GPa, the single-crystal quality deteriorates rapidly.

The single-crystal structure refinements performed at pressures of 0.12, 0.91, 2.27, and 2.79 GPa indicate (Table 4) that the phase transition is the result of a reorientation of the axial direction of the elongated Mn(III) octahedron (Figure 5). At pressures below the phase transition, the F1 atoms display the

(12) PeakFit 4.0 computer program; Jandel Scientific, San Raphael, CA, 1995.
(13) Gupta, S. C.; Chidambaram, R. *High-Pressure Res.* **1994**, *12*, 51−70.

Table 4. Selected Distances (Å), Angles (deg), and Polyhedron Volumes (Å^3) in the Na_3MnF_6 Structure[a]

		pressures (GPa)				
atoms	multiplicity	ambient	0.12	0.91	2.27	2.79
Mn − F1	2	2.0176(8)	2.038(9)	1.978(12)	1.915(12)	1.891(11)
Mn − F2	2	1.8621(8)	1.899(19)	1.81(2)	1.82(2)	1.790(18)
Mn − F3	2	1.8969(9)	1.887(12)	1.897(15)	1.935(15)	1.971(10)
Na1 − F1	2	2.262(1)	2.288(8)	2.224(11)	2.262(11)	2.234(10)
Na1 − F2	2	2.266(1)	2.243(13)	2.279(17)	2.264(17)	2.272(15)
Na1 − F3	2	2.302(1)	2.312(18)	2.29(2)	2.26(2)	2.208(14)
Na2 − F1b	1	2.257(1)	2.17(2)	2.30(4)	2.23(3)	2.27(3)
Na2 − F1	1	2.309(1)	2.318(10)	2.283(15)	2.331(15)	2.283(13)
Na2 − F2b	1	2.329(1)	2.324(16)	2.35(2)	2.35(2)	2.370(18)
Na2 − F3a	1	2.319(1)	2.333(14)	2.297(17)	2.257(16)	2.258(14)
Na2 − F3c	1	2.631(1)	2.64(2)	2.61(3)	2.56(3)	2.53(2)
Na2 − F2	1	2.691(1)	2.712(18)	2.62(2)	2.59(2)	2.566(19)
Na2 − F2c	1	2.847(1)	2.823(15)	2.843(19)	2.73(2)	2.718(17)
Na2 − F3	1	2.874(1)	2.864(13)	2.858(16)	2.857(17)	2.871(14)
F1 − Mn − F2	2	88.24(3)	90.2(5)	86.0(9)	89.8(8)	87.3(8)
F1 − Mn − F2a	2	91.76(3)	89.8(5)	94.0(9)	90.2(8)	92.7(8)
F1 − Mn − F3	2	88.73(3)	87.6(4)	90.1(6)	88.6(6)	89.2(5)
F1 − Mn − F3a	2	91.27(3)	92.4(4)	89.9(6)	91.4(6)	90.8(5)
F2 − Mn − F3	2	90.60(4)	91.0(7)	89.4(8)	88.9(8)	89.2(6)
F2 − Mn − F3a	2	89.40(4)	89.0(7)	90.6(8)	91.1(8)	90.8(6)
V(Mn−F_6)		9.496(4)	9.73(8)	9.05(10)	8.97(10)	8.88(8)
V(Na1−F_6)		15.597(7)	15.72(11)	15.32(14)	15.27(14)	14.76(10)
V(Na2−F_8)		26.457(9)	26.42(14)	26.05(21)	25.28(19)	25.07(17)

[a] Ambient pressure data are from English et al.[1] The symmetry codes are a, $-x, -y, -z$; b, $^1/_2 - x$, $^1/_2 + y$, $^1/_2 - z$; c, $^1/_2 + x$, $^1/_2 - y$, $^1/_2 + z$.

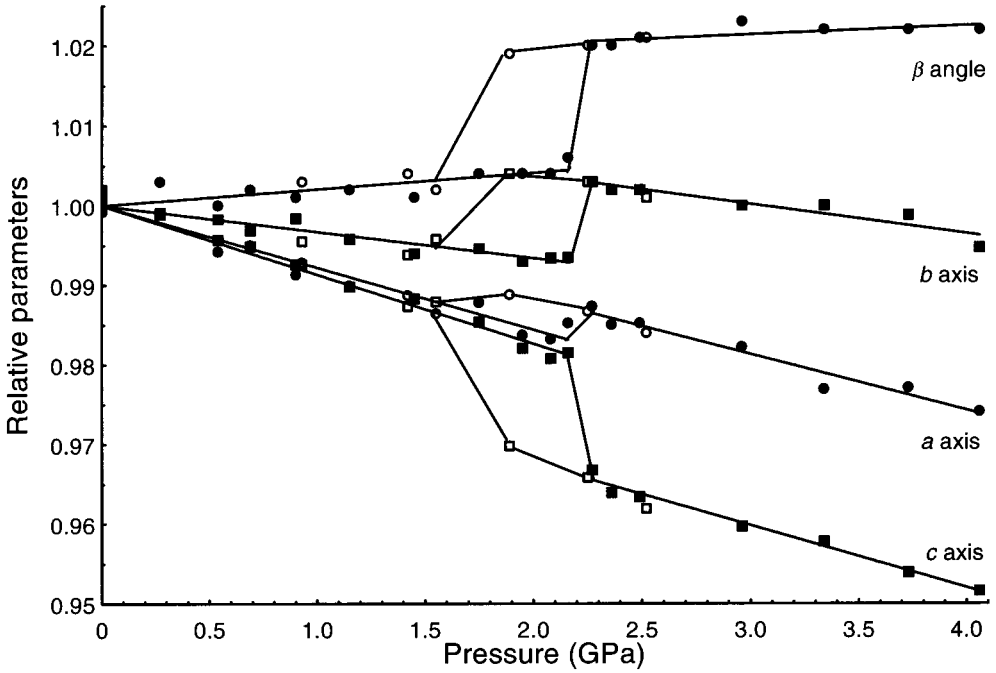

Figure 2. Relative values of the unit cell parameters of Na_3MnF_6. Filled markers indicate increasing pressure, and unfilled markers indicate decreasing pressure.

longest distances to the manganese atom, and the Mn−F1 bonds form angles of approximately ±20° to the [0 0 1] direction. Above the transition pressure, the axis of elongation for the Mn-centered coordination sphere points toward the F3 atoms and forms angles of about ±70° to [0 0 1]. The structure refinement of Na_3MnF_6 at 2.27 GPa shows that the bond distances Mn−F1 and Mn−F3 are almost equal at this pressure (Table 4), which is very close to the phase transition region. Further studies to investigate if this observed oblate distortion represents a well-ordered or intermediate disorder state have been initiated. These studies will aim at a better characterization of the structures of the phases formed in the hysteresis from about 1.7 to 2.2 GPa.

Norrestam[14] has shown that the distortion of coordination around ions such as Mn^{3+} and Cu^{2+} can be geometrically interpreted as due to a nonspherical effective shape of the ions. In these cases, the spherical model of the shape of the ion, which enables the use of the simple ion radius concept, has to be replaced by an ellipsoidal model. In a case like the present, when the coordination has an approximate D_{2h} symmetry, the effective ionic shape of Mn^{3+} is described by the expression

(14) Norrestam, R. *Z. Kristallogr.* **1994**, *209*, 99−106.

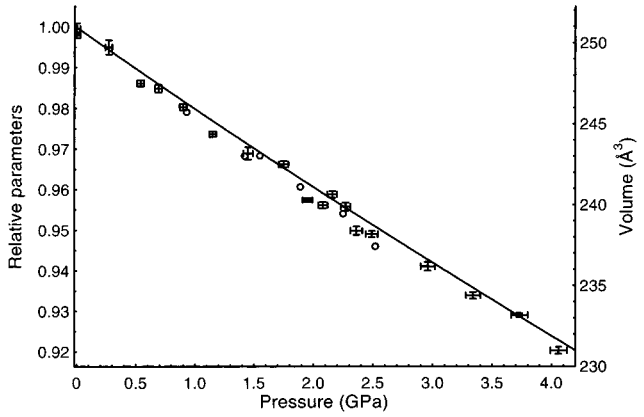

Figure 3. Change in volume versus pressure in the Na_3MnF_6 structure. Error bars indicate 2 esd's, and circles represents data when the pressure is lowered. The solid line represents a fit of the experimental unit cell volumes to the Birch equation of state.

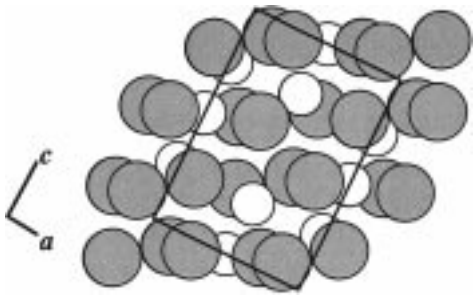

Figure 4. Packing of F^- and Na^+ ions in Na_3MnF_6, viewed along the [0 1 0] directions. The gray fluorine ions are drawn with radii 1.0 Å and the white sodium ions with radii 0.75 Å.

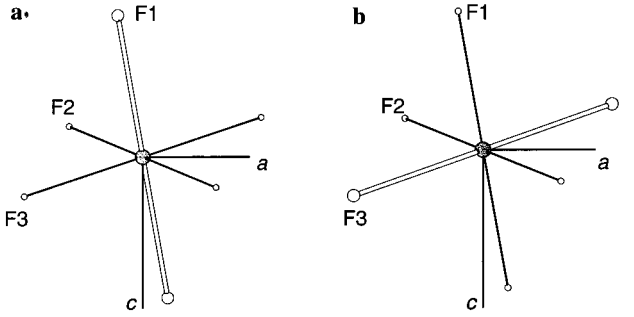

Figure 5. Axial directions (thick bonds) of the elongated manganese fluoride octahedra in Na_3MnF_6, viewed along the [0 1 0] direction, (a) before the phase transition, at ambient pressure (Mn−F1 distance 2.0176(8) Å), and (b) after the phase transition, at 2.79 GPa (Mn−F3 distance 1.975(13) Å).

$2/r_a^2 + 2/r_b^2 + 2/r_c^2 = 6/r_0^2$. In this expression, r_a, r_b, and r_c are the effective radii along the principal axes of the ellipsoid, and r_0 can be regarded as an estimate of a spherical radius. The value of r_0, which has the advantage of being independent of the degree of distortion, is determined as the root harmonic mean square (rhms) value, viz., $1/r_0^2 = {}^1/_6\Sigma 1/r_i^2$. The six r_i values are calculated from the Mn−F bond distances d_i as $d_i - r_F$, where r_F is the ionic radius of the F^- ion. At ambient pressure, a reasonable estimate of r_F would be 1.33 Å.[15] For Mn^{3+}, the r_0 value was determined from a large number of oxides and fluorides to be 0.59(1) Å.[14]

In the present case, the bond distance data at ambient pressure give the rhms value $r_0 = 0.586$ Å for six-coordinated Mn^{3+}, in good agreement with the general value, 0.59(1) Å. When determining rhms values at nonambient conditions, the lack of knowledge of the values of the ionic radius r_F of F^- at different pressures creates problems. In this study, the compressibility of the monovalent F^- anions was considered to be dominating compared to that of the trivalent Mn^{3+} cations. Accordingly, the change of the average values of the six Mn−F bond distances with pressure was considered to be entirely due to the assumed larger compressibility of the F^- ions. With the present data, the F^- radius varied with pressure as $r_F \approx 1.33 - 0.015p$ (where p is the pressure in gigapascal). The rhms values of Mn^{3+} calculated with these F^- radii for 0.91, 2.27, and 2.79 GPa were 0.57, 0.58, and 0.58 Å, respectively, again in good agreement with the expected general value, 0.59(1) Å.

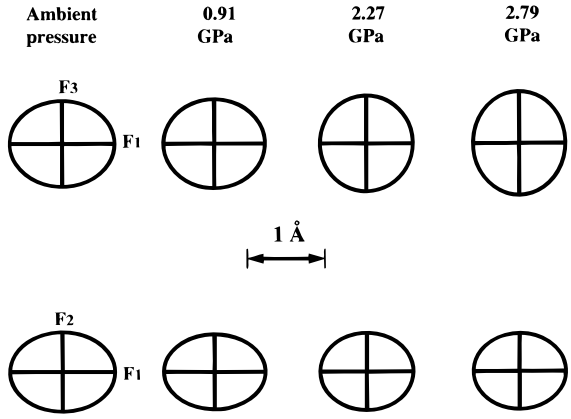

Figure 6. Effective ellipsoidal shapes of the Mn^{3+} ions as a function of pressure. Upper row shows projections of the ellipsoids approximately along the Mn−F2 bond, and the row below shows projections along the Mn−F3 bond.

The effective ellipsoidal shapes of the Mn^{3+} ions as a function of pressure, estimated from the observed bond distance data, are shown in Figure 6. This figure offers an alternative way of illustrating the changes observed over the phase transition and shows clearly how the largest principal axis describing the ellipsoidal shape flips from being directed toward the fluorine F1 position to being directed toward the F3 position. The compressed (oblate) shape of the Mn^{3+} ion at 2.27 GPa is also evident. However, to completely secure that the shapes in the hysteresis range 1.7−2.2 GPa are well defined and not affected by disorder phenomena will need further investigation.

The optical absorption spectra recorded at ambient and high pressures (2.4 GPa) show a single, broad, highly skewed and fairly intense absorption feature in the visible spectral range (Figures 7 and 8). Computer fits of the spectra reveal three relatively broad ($\omega_{1/2} = 1900-2200$ cm^{-1}), partly overlapping bands, which are centered in spectra recorded at ambient pressure at 17 490, 19 180, and 20 830 cm^{-1}. The simple 3d cation chemistry, in conjunction with width and energies of the three observed bands, allows an unequivocal assignment of these bands to spin-allowed electronic d−d transitions in trivalent manganese. In the high-pressure spectra (2.4 GPa), the bands are shifted approximately 100 cm^{-1} toward higher energies (17 660, 19 280, and 20 920 cm^{-1}), which is consistent with a general shortening of the Mn−F bonds at elevated pressures. The relatively low molar extinction coefficients ($\epsilon \leq 5$ L mol^{-1} cm^{-1}) for the spin-allowed Mn^{3+} d−d transitions indicate that the manganese ion is located in a centrosymmetric ligand field. The polarization ($E||Z(a) = E||Y(b) \gg E||X(c)$) of the absorption bands in spectra recorded at ambient conditions (Figure 7) is consistent with a $3d^4$ cation in a ligand field of D_{2h} symmetry with the C_2-axis of the field slightly inclined to the optical X direction (c-axis). The absorption spectra of an $X'(c')$-$Z(a)$

(15) Shannon, R. D. *Acta Crystallogr.* **1976**, *A32*, 751−767.

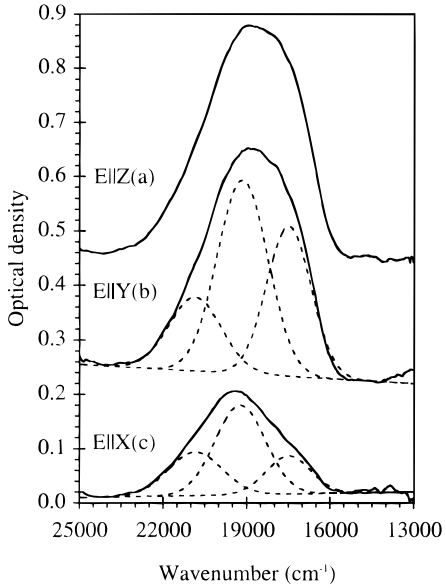

Figure 7. Optical absorption spectra of Na_3MnF_6 for *E* polarized along the three optical main axes *X*, *Y*, and *Z*. The measured spectra (full lines) were obtained at ambient conditions on a 36-μm-thick single crystal. For the sake of readability, the $E||X$ and $E||Y$ spectra have been offset 0.22 and 0.44 units from the baseline. Dashed lines beneath the $E||X$ and $E||Y$ spectra represent curve-resolved Gaussian band components. The deconvolution result for $E||Z$, which is not included in this figure, is essentially equal to that of $E||Y$.

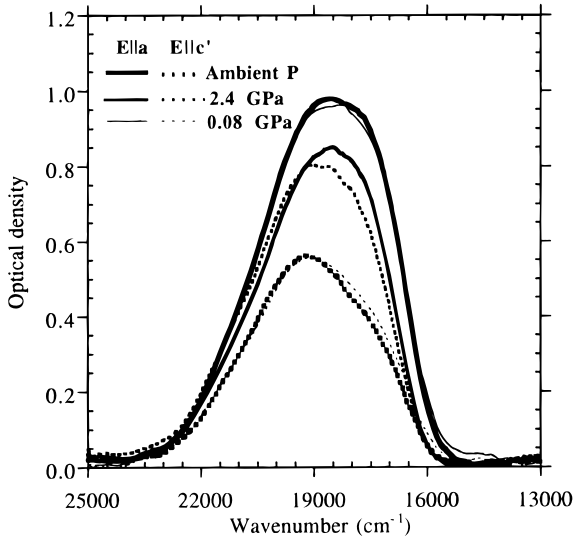

Figure 8. Polarized optical absorption spectra of an 80-μm-thick Na_3MnF_6 single crystal at ambient pressure and at 0.08 and 2.40 GPa. Solid lines indicate $E||a$ and dotted lines $E||c'$.

single-crystal section measured at high pressure reveal negligible dichroism, and the intensities of the three recorded Mn^{3+} bands are of almost equal intensities for the two vibrational directions, $E||X'(c')$ and $E||Z(a)$ (Figure 8). When releasing the pressure below the transition range, the original dichroism of the single-crystal platelet is restored, and the polarized optical spectra are essentially identical to those recorded at ambient conditions prior to the high-pressure experiment (Figure 8). In other words, the spectacular polarization change which is observed when passing the transition pressure is a reversible effect ($E||a \gg E||c \leftrightarrow E||a = E||c$). This unusual polarization change is consistent with a reorientation of the $z(C_2)$-axis of the ligand field at the Mn(III) ion at high pressures from $z \approx c$ to $z \approx b$ and, thus, further corroborates the results and the interpretations of the x-ray single-crystal refinements.

High-pressure x-ray investigations of the structurally isotypic fluoride Na_3ScF_6 show similar compressibilities of the unit cell dimensions as for Na_3MnF_6, but no phase transition of the presently recorded character has been found in the pressure range from ambient conditions to 6.82 GPa.[16] This confirms that the high-pressure phase transition in Na_3MnF_6 is primarily caused by the electron configuration of trivalent manganese ($3d^4$), which is susceptible to Jahn−Teller effects. The decrease in polyhedral volume at the manganese(III) site from ambient conditions to 2.79 GPa is 6%, while the volume decrease for the NaF_6 and NaF_8 polyhedra is approximately 5%. In Na_3ScF_6, the polyhedral volume decrease in the same pressure range is drastically different, showing a very small ScF_6 volume change of 1% and a significantly larger volume decrease (7−8%) for the two different sodium polyhedra. The recorded relative change in unit cell volume versus pressure for Na_3MnF_6 has, as shown in Figure 3, been fitted to the Birch type equation of state[17]

$$P = {}^3/_2 B_0(x^{-7/3} - x^{-5/3})[1 - {}^3/_4(4 - B_0')(x^{-2/3} - 1)]$$

where x is the relative volume, V/V_0, and P is pressure. The isothermal bulk modulus at ambient pressure, B_0, and its derivative with respect to pressure, B_0', were determined to 47.8-(1) GPa and 1.2(1), respectively.

As discussed above, the structure could be considered as a layered packing of low-charged Na^+ and F^- ions along [1 0 $\bar{3}$]. The distortions of the MnF_6 octahedra can easily be accommodated in the structure when the distortions are directed out from the layers. When the pressure is increased, the interlayer distances decrease rapidly, and such an arrangement might become less favorable. At higher pressures, it may become easier to accommodate the distortions within the planes of packing. At ambient pressure, the distortion directions (elongations) defined by the Mn−F1 vectors have an angle of 49° with the normal to the [1 0 $\bar{3}$] planes. The Mn−F2 and Mn−F3 vectors form angles of 65° and 69° with the [1 0 $\bar{3}$] normal, respectively. Thus, assuming, as above, that the distortions at higher pressures might be more favorably accommodated within the planes of packing, it is reasonable to expect that the elongation would switch from the least favorable Mn−F1 to the most favorable Mn−F3 direction. It is, of course, tempting to assume that, eventually, when raising the pressure, the Mn−F1 distance would become the shorter one. The similar angles that Mn−F2 and Mn−F3 form with the packing direction might imply that a configuration where the Mn−F2 and Mn−F3 distances are more equal becomes favorable. Thus, one might expect a second transition from prolate (4 + 2) coordination around Mn(III) to an oblate (2 + 4) one. The strains induced when having to accommodate two different distortions within the layers might, thus, be the reason for the sudden collapse of the monocrystal.

Conclusions

The existence of a reversible, isosymmetric, high-pressure phase transition at 1.7−2.2 GPa in Na_3MnF_6 has been demonstrated by means of single-crystal x-ray structure refinements using DAC techniques. The transition involves a flip of the elongation axis of the Mn(III)-centered coordination octahedra from an orientation approximately along the *c*-axis to an orientation close to the *b*-axis. To our knowledge, this is the first example of a pressure-induced, reversible transition due to a flip of the Jahn−Teller distortion directions around Mn^{3+}

(16) Carlson, S.; Xu, Y.; Norrestam, R. *J. Solid State Chem.*, in press.
(17) Birch, F. *J. Geophys. Res.* **1952**, *57*, 227.

that has been possible to characterize by single-crystal diffraction methods. Polarized single-crystal absorption spectra at ambient and elevated pressures (2.4 GPa) show strong, reversible polarization effects of absorption bands due to spin-allowed d−d transitions in trivalent manganese, which are consistent with the structure refinement results. The phase transition shows a 0.5-GPa-wide hysteresis region which needs to be further investigated. A study aiming at a detailed characterization of the structure of phases formed in this pressure interval has been initiated. The experiments have also shown a collapse of the single crystals, occurring at 4.06 GPa. The above-mentioned phase transitions at 1.7−2.2 GPa can be explained as due to a change of the distortions, from being directed along the directions of highest compressibility to be aligned along directions with lower compressibility. The collapse of the crystals at higher pressures might be due to a transition from prolate (2 + 4) to oblate (4 + 2) distortions of the MnF_6 octahedra, with all four elongated Mn−F bonds aligned along lower compressibility directions, viz., within the layers of packing.

Acknowledgment. We are indebted to the Swedish National Research Council for the grants that enabled this investigation and the participation of one of the authors (Y.X.). We also thank Arne Sjödin for assisting in the synthetic work.

Supporting Information Available: Tables I−IV, containing observed and calculated structure factors (with standard deviations) for the structure determinations performed at 0.12, 0.91, 2.27, and 2.79 GPa (4 pages). An X-ray crystallographic file, in CIF format, is also available on the Internet only. Ordering and access information is given on any current masthead page.

IC971171G